Growth of (Y[1−x] Ca[x])Ba[2]Cu[4]O[8] in ambient pressure and its tri-axial magnetic alignment

AUTHOR(S):

Horii, S; Yamaki, M; Shimoyama, J; Kishio, K; Doi, T

CITATION:

Horii, S ...[et al]. Growth of (Y[1−x] Ca[x])Ba[2]Cu[4]O[8] in ambient pressure and its tri-axial magnetic alignment. Superconductor Science and Technology 2015, 28(10): 105003.

ISSUE DATE:

2015-10-01

URL:

http://hdl.handle.net/2433/202565

Growth of $(Y_{1-x}Ca_x)Ba_2Cu_4O_8$ in ambient pressure and its tri-axial magnetic alignment

S Horii[1 *], **M Yamaki**[2], **J Shimoyama**[3], **K Kishio**[4], and **T Doi**[1]

[1] Graduate School of Energy Science, Kyoto University, Yoshida-Honmachi, Sakyo-ku, Kyoto 606-8501, Japan
[2] Department of Environmental Systems Engineering, Kochi University of Technology, Tosa-Yamada, Kami-shi, Kochi 782-8502, Japan
[3] Department of Physics and Mathematics, Aoyama Gakuin University, Fuchinobe, Chuo-ku, Sagamihara-shi, Kanagawa 252-5258, Japan
[4] Department of Applied Chemistry, University of Tokyo, Hongo, Bunkyo-ku, Tokyo 113-8656, Japan

E-mail: horii.shigeru.7e@kyoto-u.ac.jp

Abstract. We report the growth of single crystals in ambient pressure and tri-axial orientation under modulated rotation magnetic fields (MRFs) for $(Y_{1-x}Ca_x)Ba_2Cu_4O_8$ [$(Y_{1-x}Ca_x)124$] with $x \leq 0.1$. Rectangular $(Y_{1-x}Ca_x)124$ crystals with approximately 50 μm in size have been successfully grown for $x \leq 0.1$ in a growth temperature region from 650°C to 750°C. Their critical temperatures increased with x and exhibited approximately 91 K for $x = 0.1$. By applying an MRF of 10 T, pulverised powders of $(Y_{1-x}Ca_x)124$ were tri-axially aligned in epoxy resin at room temperature in a whole x region below $x = 0.1$. The magnitude relationship of the magnetic susceptibilities (χ) along crystallographic directions for $(Y_{1-x}Ca_x)124$ was $\chi_c > \chi_a > \chi_b$ at room temperature and was unchanged with a change in x. From changes in the degrees of the c-axis and the in-plane orientation ($\Delta\omega$) for the $(Y_{1-x}Ca_x)124$ powder samples aligned under three different MRF conditions, it was found that MRFs above at least 1 T were required to achieve almost complete tri-axial alignment with $\Delta\omega < 5°$. Irreversibility lines for $H//c$ were successfully determined even from the powder samples by the introduction of magnetic alignment without using single crystalline samples. The present study indicates that magnetic alignment is a useful process for the fabrication of quasi-single-crystals from the perspective of solid-state physics and the production of cuprate superconducting materials.

1.Introduction

The rare-earth (RE)-based cuprate superconductor $REBa_2Cu_3O_y$ (RE123) has a 90 K-class critical temperature (T_c) [1], and its T_c is higher than the boiling temperature of liquid nitrogen (77.3 K). A T_c of ~ 90 K in RE123 is in an optimally carrier-doped condition, which is achieved with almost a full oxidation process for RE123 compounds. As compared to another practical cuprate superconductor, $(Bi,Pb)_2Sr_2Ca_2Cu_3O_y$ [2], RE123 with y ~ 7 exhibits intrinsically higher critical current properties under high magnetic fields at 77 K. Therefore, RE-based cuprates are candidates for superconducting materials to be used for practical applications using superconducting bulk magnets [3] and cables for high-field solenoidal magnets [4].

In addition to the research and development cited above for the practical use of RE123, basic experimental studies have also been carried out on the RE-Ba-Cu-O system. It has been well established that three superconducting phases exist in the RE-Ba-Cu-O system: RE123 ($6 < y < 7$), $RE_2Ba_4Cu_7O_y$ (RE247, $14 < y < 15$) [5], and $REBa_2Cu_4O_8$ (RE124) [6]. All of them are characterised by the layered perovskite structure, which is an anisotropic crystal structure with a stacked structure alternating two-dimensional superconducting CuO_2 plane and a one-dimensional blocking chain along the direction of the c-axis. The structural differences in

these three compounds originate from the differences in the stacking sequences of the Cu-O chains: the repetition of a single-chain, that of the double-chain, and the alternate repetition of a single- and double-chain for RE123, RE124, and RE247, respectively.

As examples, the crystal structures of $YBa_2Cu_3O_y$ (Y123, y = 7, T_c ~ 92 K) and $YBa_2Cu_4O_8$ (Y124, T_c ~ 81 K) are shown in Fig. 1. Fully oxidised Y123 consists of bilayered CuO_2 planes and a single Cu-O chain in a unit cell. This layered crystal structure induces anisotropic physical properties, and the critical current density (J_c) parallel to the superconducting CuO_2 plane (// *ab*-plane direction) is superior to the J_c parallel to the *c*-axis [7]. As shown in Fig. 1(b), Y124 possesses a double Cu-O chain without oxygen nonstoichiometry as the blocking layer in its crystal structure. This is quite different from Y123 containing single chains with oxygen nonstoichiometry [8]. The structurally rigid double Cu-O chain in RE124 and RE247, which runs parallel to the *b*-axis, preserves an orthorhombic phase for the temperature change to room temperature after the synthesis process, resulting in the generation of twin-free grains. Incidentally, in the case of practical RE123 materials, structural transition [9, 10] to an orthorhombic phase from a tetragonal phase due to the increase in y generally induces the generation of twin microstructures in the *ab*-plane direction [11].

In addition to the layered crystal structures, the symmetry of superconducting Cooper pairs based on the *d*-wave [12] and short coherence length along the CuO_2 plane direction should also be taken into account for the practical use of cuprate superconductors. The increase in the misorientation angle between two Y123 grains leads to serious reduction of the intergrain J_c parallel to the *ab*-plane direction, even for the *c*-axis-oriented Y123 grains [13, 14]. This strongly suggests that the simultaneous achievements of the formation of a *c*-axis grain-oriented microstructure and the alignment of grains along the *a*- and *b*-axis directions parallel to the CuO_2 planes are required to improve the critical current properties of cuprate superconductor materials for practical applications. Therefore, the formation of a bi- or a tri-axial grain-oriented microstructure is a key issue for the development of RE-based superconducting materials with high J_cs. At the current stage, the standard process for achieving bi-axially oriented microstructures has been thin film growth [15] on highly oriented substrates and melt solidification [16] using seed crystals, on the basis of an epitaxial growth technique.

Magnetic alignment is a candidate for being a useful grain orientation technique. Recent developments in superconducting solenoidal magnets brought us a 10 T class of static magnetic fields at a room temperature bore without the operation using liquid helium [17, 18]. High magnetic fields of ~10 T can provide kinetic and orientation energy comparable to gravity and thermal energy at room temperature, even for feeble magnetic (paramagnetic or diamagnetic) substances [19]. Furthermore, magnetic alignment is a tri-axial grain orientation technique [20–23]; simultaneous alignment of both the easy and hard axes of magnetisation is achieved by the introduction of a modulated rotation magnetic field (MRF).

This magneto-scientific crystal orientation process is a novel candidate for the formation of tri-axially oriented microstructures in cuprate superconductors. In practice, our group has reported the tri-axial orientation with the in-plane and *c*-axis orientations of less than 5° for RE247 [22, 23] and RE124 [24] powders aligned in epoxy resin under the 10 T class of MRFs at room temperature. However, in the case of RE123 as a practical superconducting material, the existence of twin microstructures, which are generated parallel to the CuO_2 plane direction, probably leads to a serious reduction of in-plane magnetic anisotropy in a grain level of RE123. Therefore, a synthesis technique of the Y124 phase at ambient pressure, which has been reported by Song *et al*. [25, 26], is fascinating as a practical use of the Y124 compound from the perspective of fabricating high-J_c Y-Ba-Cu-O materials by magnetic alignment. Although a high-oxygen-pressure synthesis method at oxygen pressures of more than 100 atm was thought to be indispensable for the easy synthesis of Y124 polycrystals [5, 27, 28], the appropriate choice of flux medium and a lower growth temperature in a flux method enabled the growth of small Y124 single crystals at ambient pressure [25]. However, the T_c (~ 81 K) for

Y124 is approximately 10 K lower than that for Y123 (y ~ 7) and has only ~ 4 K of a temperature margin as compared to the boiling point of liquid nitrogen. That is, the enhancement of T_c for Y124 is recognised as a practical issue, and the doping of calcium (Ca) into Y124 [29] is a strategy for increasing the T_c of the 124 system. Furthermore, also from the viewpoint of solid-state physics for the carrier-doped one-dimensional Cu-O chain without oxygen nonstoichiometry, the tri-axial grain orientation of the Ca-doped Y124 with different carrier-doping levels is useful as a sample preparation technique for measuring nuclear magnetic resonance.

Based on the above background, in the present study, we attempted to synthesise $(Y_{1-x}Ca_x)Ba_2Cu_4O_8$ [$(Y_{1-x}Ca_x)124$] with various Ca-doping levels, x, by optimising the growth temperature in the flux method to enhance the T_c of the 124 system. Using pulverised $(Y_{1-x}Ca_x)124$ powders, alignment of the magnetic tri-axial in epoxy resin at room temperature under the MRF of 10 T was performed to clarify the change in the magnetisation axes as a function of x. From the magnetic alignment under three different MRF conditions, a rough determination of the magnitude relationship of tri-axial magnetic anisotropies in $(Y_{1-x}Ca_x)124$ was attempted by evaluating the degrees of the in-plane and c-axis orientation using an X-ray rocking curve measurement.

2. Experimental details

Single crystals of $(Y_{1-x}Ca_x)124$ (x = 0. 0.025, 0.05, 0.075, and 0.1) were grown by the flux method [24, 25, 30] in air using KOH as a flux medium. Precursor powders consisting of (Y,Ca)123 and CuO were prepared by a solid-state reaction at 850°C in air using Y_2O_3, $CaCO_3$, $BaCO_3$, and CuO as the starting materials with an intermediate grinding. A precursor powder of (Y,Ca)123 + CuO was mixed with KOH at a weight ratio of powder : KOH = 5 : 6 and heat-treated in an Al_2O_3 crucible. The temperature for crystal growth, T_k, was maintained for 4 h prior to a slow cooling process with a cooling rate of 1°C/h. Then, furnace cooling to room temperature was performed after the slow cooling process for 100 h. The resultants were washed with distilled water several times to remove the flux, and the grown crystals were separated using filter paper. The phases of thusly grown crystals with rectangular plates with 50~100 μm in a side were identified by X-ray diffraction (XRD) analysis. To prepare fine powders of $(Y_{1-x}Ca_x)124$, a ball-milling process was performed for 3 h in ethanol using zirconia balls as a pulverisation media by a planetary mill. A secondary electron image of the pulverised powders of $(Y_{1-x}Ca_x)124$ (x = 0.1) is shown in Fig. 2(a) as an example. Platelet grains with shapes distorted and crushed by the ball-milling process can be clearly seen. Consequently, the mean diameters of the pulverised powders, which were determined from secondary electron images, were roughly 3 ~ 5 μm for $(Y_{1-x}Ca_x)124$.

The ball-milled $(Y_{1-x}Ca_x)124$ powder was mixed with epoxy resin at a weight ratio of powder : resin = 1 : 10. The epoxy resin containing the powder was cured for more than 12 h at room temperature under three different MRF conditions. As schematically shown in Fig. 2(b), the powder samples were horizontally rotated at two different steps in a static field (H_a) applied along the transverse direction. At angles of 0 and 180°, the $(Y_{1-x}Ca_x)124$ powder sample was rested for 2 s, whilst the rotation process with Ω = 60 rpm was applied to other angle regions. The original angle of the sample, 0°, was defined with regard to the direction normal to the α plane [see Fig. 2(b)] of the sample, which was parallel to the transverse H_a direction. The applied static magnetic fields were $\mu_0 H_a$ = 1, 5, and 10 T.

XRD measurements using a CuKα incident beam were performed at the α, β, and γ planes [see Fig. 2(b)] for the cured resins containing magnetically aligned $(Y_{1-x}Ca_x)124$ powders. The first easy, second easy, and hard axes for magnetisation were determined from XRD patterns at the α, β, and γ planes, respectively, of the $(Y_{1-x}Ca_x)124$ powder samples oriented in the MRF of 10 T. To determine the degrees of the c-axis and in-plane orientation for the

magnetically aligned powder samples of $(Y_{1-x}Ca_x)124$, X-ray rocking curves were examined using diffraction peaks of (00$\underline{14}$) and (200) for the tilt of the samples to the *a*- and *b*-axis directions, respectively. The full width at half maximum for each X-ray rocking curve, $\Delta\omega$, was obtained as the degree of orientation for a magnetically aligned powder sample.

The magnetic susceptibility (χ) was measured in zero-field-cooling (ZFC) and field-cooling (FC) conditions using a SQUID magnetometer at temperatures below 95 K under applied magnetic fields (H) of $\mu_0 H$ = 0.5, 1, 3, and 5 T. The Meissner effect was checked in the ZFC condition under $\mu_0 H$ = 0.1 mT, and the T_c was defined as the onset of the diamagnetisation.

3. Results and discussion

XRD measurements of powders were performed for the resultants that were obtained in the crystal growth of $(Y_{1-x}Ca_x)124$ (x = 0. 0.025, 0.05, 0.075, and 0.1) at various T_ks, and XRD patterns for the resultants grown at T_k= 750°C are shown in Fig. 3 as an example. Almost all of the diffraction peaks for the five XRD patterns in Fig. 3 were identified as reflections of the Y124 structure, indicating that the flux method using KOH enables crystal growth at the Y124 phase even in air.

To clarify the relationship between T_k and the obtained phases, a phase diagram for the change in T_k as a function of the nominal Ca-doping level (x) in $(Y_{1-x}Ca_x)124$ is shown in Fig. 4. In the case of x = 0, the T_k range in which the 124 phase could be grown was found to be from 660°C to 800°C. However, Y123 and a mixture of non-layered-perovskite phases were obtained at higher and lower T_ks, respectively, as compared to the T_k range required for the synthesis of Y124. In the case of the Ca-doped Y124, the 124 phase was obtained for 650°C ≤ T_k ≤750°C; this result roughly suggests that the T_k range for the synthesis of the 124 phase was almost constant for the change in x.

For a rough determination of the Ca-doping levels for thusly obtained $(Y_{1-x}Ca_x)124$ crystals, the temperature dependence of the magnetic susceptibility (χ) under $\mu_0 H$= 0.1 mT was obtained for the five samples of $(Y_{1-x}Ca_x)124$ (T_k= 750°C) in the ZFC condition. The χ - T curves for $(Y_{1-x}Ca_x)124$ are shown in Fig. 5(a). Clearly, all five samples exhibited strong diamagnetisation; therefore, the grown $(Y_{1-x}Ca_x)124$ samples were bulk superconductors. Furthermore, it was found that the T_c increased with an increase in nominal x. Figure 5(b) shows the x dependence of the T_c for the $(Y_{1-x}Ca_x)124$ crystals, together with data for the polycrystalline $(Y_{1-x}Ca_x)124$ samples synthesised by solid-state reaction under ambient [31] and high-oxygen pressures [29], for reference. The T_c values in the present study systematically increased with the increase in nominal x for $x \leq 0.075$, and T_c reached ~ 91 K for x = 0.075. For $x \geq 0.075$, the T_c was almost saturated. However, as shown in Fig. 5(a), the diamagnetic χ - T curve below T_c for x = 0.075 was relatively broadened as compared to that for x = 0.1. This strongly suggests that the Ca-doping levels for the obtained 124 crystals are inhomogeneous in the case of x = 0.075. When the values of the T_c were compared with those reported by Zheng *et al*. [31] and Miyatake *et al*. [29], the T_cs for x = 0, 0.025, 0.05, and 0.1 in the present study were found to coincide well with those in the two studies. One can recognise that the Ca-doping levels are controlled by the nominal composition and are almost coincident with nominal x, even for the $(Y_{1-x}Ca_x)124$ crystals grown by the flux method.

Using the pulverised powders of thusly obtained $(Y_{1-x}Ca_x)124$ crystals, the magnetically oriented powder samples of $(Y_{1-x}Ca_x)124$ were fabricated under MRFs of 1, 5, and 10 T in epoxy resin at room temperature. The XRD patterns at the α, β, and γ planes for the $(Y_{1-x}Ca_x)124$ (x = 0, 0.05, and 0.1) powder samples oriented in the MRF of 10 T are shown in Figs. 6(a), 6(b), and 6(c), respectively. As shown in Fig. 6(a), in the case of x = 0, the (00l), (h00), and (0k0) peaks are clearly enhanced at the α, β, and γ planes, respectively. This result means that the powders of Y124 were tri-axially oriented under the MRF of 10 T, and the

relationship of the magnetisation axes was $\chi_c > \chi_a > \chi_b$ for $(Y_{1-x}Ca_x)124$ (x = 0), which is consistent with the results our group previously reported [32]. As can be clearly seen from Figs. 6(b) and 6(c), the XRD patterns for the magnetically aligned powder samples with x = 0.05 and 0.1 were almost identical to the XRD patterns in Fig. 6(a). Note that these results were obtained also for x = 0.025 and 0.075. Consequently, it was found from the XRD measurements of the magnetically oriented powder samples of $(Y_{1-x}Ca_x)124$ (x = 0, 0.05, and 0.1) that an almost complete tri-axial orientation was accomplished for all of the pulverised $(Y_{1-x}Ca_x)124$ powders under the MRF of 10 T, and the relationship of the magnetisation axes ($\chi_c > \chi_a > \chi_b$) was unchanged with a change in x.

For the purpose of evaluating the degrees of in-plane and c-axis orientation, X-ray rocking curves were measured for all $(Y_{1-x}Ca_x)124$ powder samples oriented in MRFs under $\mu_0 H_a$ = 1, 5, and 10 T. As an example of the H_a-dependent degrees of the c-axis and in-plane orientations, X-ray rocking curves at the (00$\underline{12}$) and (200) peaks in the $(Y_{1-x}Ca_x)124$ (x = 0.1) powder samples oriented under the MRFs of 1, 5, and 10 T are shown in Figs. 7(a) and 7(b), respectively. It should be noted that the tilt of the samples to the a-axis and b-axis directions was performed in the rocking curve measurement to determine the degrees of the c-axis and in-plane orientations, respectively. In the case of the c-axis orientation in Fig. 7(a), the $\Delta\omega$ values in the rocking curves for x = 0.1 were slightly broadened with a decrease in $\mu_0 H_a$. However, these three rocking curves exhibited $\Delta\omega$ < 3°. This strongly indicates that high degrees of the c-axis orientation for $(Y_{1-x}Ca_x)124$ (x = 0.1) powders were accomplished even in magnetic alignment under the MRF of 1 T. On the other hand, in the case of the in-plane orientation in Fig. 7(b), the $\Delta\omega$ values were found to be sensitive to the strength of the applied magnetic field in MRF. In detail, the values of $\Delta\omega$ and the peak intensity for the rocking curves were drastically broadened and weakened, respectively, with a decrease in $\mu_0 H_a$. The determined $\Delta\omega$ values were ~9°, ~3.5°, and ~2° for $\mu_0 H_a$ = 1, 5, and 10 T, respectively. Consequently, tri-axial magnetic alignment with the high c-axis and in-plane orientation degrees with $\Delta\omega$ < 2° in the MRF of 10 T for the powders of Ca-doped Y124 with T_c = 91 K could be achieved as a proof-of-principle of the tri-axial magnetic alignment technique.

The changes in $\Delta\omega$ as a function of x are plotted in Figs. 8(a) and 8(b) to clarify the x-dependent c-axis and in-plane orientation degrees, respectively. A striking feature in Fig. 8(a) is that high degrees of the c-axis orientation with $\Delta\omega$ < 1.5° were accomplished for all aligned $(Y_{1-x}Ca_x)124$ powder samples in the case of MRFs under $\mu_0 H_a$ = 10 T. Furthermore, the $\Delta\omega$ values reached $\Delta\omega$ < 2° for the MRF of 5 T and maintained $\Delta\omega$ < 5° even for the MRF of 1 T. That is, the changes in $\Delta\omega$ as a function of the applied transverse magnetic field in the MRF were roughly constant. Within the results in the present study, the result in Fig. 8(a) probably indicates that a remarkable change in the c-axis magnetic anisotropy (χ_c-χ_a) does not appear for a change in x, and the c-axis magnetic anisotropies were sufficient for grain orientation under the MRF of 1 T. Namely, even the c-axis magnetic anisotropy generated by the Cu ions at the CuO_2 planes and Cu-O double chains was sufficient to achieve an almost complete c-axis orientation in the MRF of 1 T.

As shown in Fig. 8(b), the degree of in-plane orientation showed an insensitive behaviour to the Ca-doping level as well; however, the $\Delta\omega$ values were relatively more sensitive to the applied transverse magnetic field in the MRF as compared with the results in Fig. 8(a). Particularly, although high degrees of the c-axis orientation with $\Delta\omega$ ~ 2° were accomplished for all of the aligned $(Y_{1-x}Ca_x)124$ powder samples in the case of the MRF of 10 T, the MRF of 1 T was clearly insufficient for achieving high degrees of in-plane orientation in the whole x region. To improve the in-plane orientation degree under lower magnetic fields, introduction of higher Ω and/or doping of heavy RE ions, such as Dy and Ho, with higher tri-axial magnetic anisotropies [33, 34] are required.

Finally, irreversibility lines of $(Y_{1-x}Ca_x)124$ (x = 0, 0.05, and 0.1) for H//c are shown

in Fig. 9 as an example of the clarification of anisotropic functionality using tri-axially aligned powder samples. It should be noted that the reduced temperature, which is normalised by T_c, T/T_c, is expressed as an abscissa of Fig. 9; and the irreversibility temperatures were determined from the temperature dependences of magnetic susceptibilities in ZFC and FC conditions. Incidentally, the ILs for a twin-free Y123 single crystal [35] and $(Y_{1-x}Ca_x)124$ films [30] were also shown for reference, and these ILs as a function of T/T_c in Fig. 9 were replotted from both the T_c values and the $\mu_0 H_{irr}$-T plots in these reports [30, 35]. From the data in the present study, it was found that the ILs were shifted toward the higher T and H regions with an increase in x. This tendency was qualitatively consistent with the result for epitaxially grown $(Y_{1-x}Ca_x)124$ films, indicating that Ca-doping into Y124 is obviously effective for increasing not only the T_c but also the vortex pinning potential under $H//c$. In the case of a Y123 superconductor with oxygen nonstoichiometry, H_{irr} was reported to be clearly improved with the increase in the oxygen content of Y123 [36]. Furthermore, the ILs of Y123 were sensitive to slight changes in y, even at the optimal carrier-doping level, and, specifically, the $\mu_0 H_{irr}$ values were drastically reduced from ~ 8 T to 4 T with the slight decrease of $\Delta y \sim 0.1$ from the optimal carrier-doped condition [35]. The behaviour of the ILs in the present study is qualitatively consistent with the relationship between the optimal carrier-doping level and $\mu_0 H_{irr}$ in Y123.

On the other hand, despite the optimal carrier-doped samples with almost the same T_cs of 91 ~ 92 K, the IL for x = 0.1 was located remarkably lower in the T and H regions as compared to the IL of the twin-free Y123 crystal. At the current stage, the origin of the relatively lower H_{irr} in $(Y_{1-x}Ca_x)124$ (x = 0.1) has been unclear. As suggested from the χ-T curves in Fig. 5(a), the crystals for x = 0.1 show a broad diamagnetic signal with $\Delta T_c \sim 5$ K. It is likely that one of the reasons is that the inhomogeneous T_c distribution induced by the fluctuating Ca-doping levels is dependent on crystals in the resultants. In these cases, the optimisation of growth conditions, such as the T_k, cooling rate, and nominal x, for the fabrication of $(Y_{1-x}Ca_x)124$ crystals with a homogeneous T_c distribution with T_c = 91 K is required. However, in the present study, the tri-axial magnetic alignment for the Y124 compound with a 90-K class of T_c has been successfully achieved, and the intrinsic improvement of vortex-pinning properties by Ca-doping could be clarified even from the tri-axially oriented powder samples. Furthermore, also from the perspective of solid-state physics for the carrier-doped one-dimensional Cu-O chain without oxygen nonstoichiometry, it is expected that the tri-axial grain orientation of the Ca-doped Y124 with different carrier-doping levels is useful as a sample preparation technique for measuring nuclear magnetic resonance.

4. Summary

We demonstrated the crystal growth of Ca-doped Y124 in ambient pressure and the tri-axial orientation of their ball-milled powders at room temperature under three different MRF conditions. $(Y_{1-x}Ca_x)124$ crystals with $x \leq 0.1$ were successfully grown in the T_k region of 650°C ≤ T_k ≤ 750°C and showed a positive x-dependence of the T_c for crystals grown at T_k = 750°C. Consequently, the T_c reached ~91 K for x = 0.1, and the Ca-doping levels in $(Y_{1-x}Ca_x)124$ crystals could be controlled by a nominal composition of x.

All pulverised $(Y_{1-x}Ca_x)124$ powders obtained in the present study were tri-axially aligned under an MRF of 10 T in epoxy resin at room temperature, and their c-axis and in-plane orientation degrees showed $\Delta\omega < 2°$. The relationship of their magnetisation axes was $\chi_c > \chi_a > \chi_b$ and was unchanged by a change in x for $x \leq 0.1$. From the degrees of the c-axis and in-plane orientations for $(Y_{1-x}Ca_x)124$ powder samples oriented in the MRFs of 1 and 5 T, it was found in the whole x region that the degrees of c-axis orientation were insensitive to $\mu_0 H_a$, whilst the in-plane orientation degrees were drastically reduced with a decrease in $\mu_0 H_a$. This roughly means that remarkable changes in the tri-axial magnetic anisotropies were not observed

in $(Y_{1-x}Ca_x)124$, and the MRFs with $\mu_0 H_a > 1$ T at least are required for the achievement of the almost complete tri-axial alignment of $(Y_{1-x}Ca_x)124$ grains with 3~5 μm in size.

Using the tri-axially aligned $(Y_{1-x}Ca_x)124$ powder samples ($\mu_0 H_a$ =10 T), the ILs for $H//c$ were determined from the magnetisation measurement. An intrinsic increase in the critical current properties of Y124 for $H//c$ by Ca-doping could be clarified from $(Y_{1-x}Ca_x)124$ powders without single crystalline bulks. The present study revealed that the tri-axial grain alignment of the 124 phase with T_c ~91 K was achieved by introducing the MRF, and the magnetic alignment is a strong tool for fabricating quasi-single-crystals from the perspective of solid-state physics and the production of cuprate superconducting materials.

5. Acknowledgments

This work was partly supported by the Nippon Sheet Glass Foundation for Materials Science and Engineering, the Iwatani Naoji Foundation, and a Grant-in-Aid for Scientific Research (No. 24550236) from JSPS, Japan. The authors thank Mr Takayuki Nishikawa for their kind support in sample preparation.

REFERENCES

[1] Dimos D, Chaudhari P, Mannhart J and LeGoues F K 1988 *Phys. Rev. Lett.* **61** 219.
[2] Laibowitz R B, Koch R H, Chaudhari P and Gambino R J 1987 *Phys. Rev. B* **35** 8821
[3] Chen Y L, Chan H M, Harmer M P, Todt V R, Sengupta S and Shi D 1994 *Physica C* **234** 232
[4] Kimura T, Kimura F and Yoshino M 2006 *Langmuir* **22** 3464
[5] Jorgensen J D, Veal B W, Kwok W K, CrabtreeG W, Umezawa A, Nowicki L J and Paulikas A P 1987 *Phys. Rev. B* **36** 5731
[6] Kishio K, Shimoyama J, Hasegawa T, Kitazawa K and Fueki K 1987 *Jpn. J. Appl. Phys.* **26** L1228
[7] Fukushima T, Horii S, Ogino H, Uchikoshi T, Suzuki T S, Sakka Y, Shimoyama J and Kishio K 2008 *Appl. Phys. Express* **1** 111701
[8] Horii S, Ishihara A, Fukushima T, Uchikoshi T, Ogino H, Suzuki T S, Sakka Y, Shimoyama J and Kishio K 2009 *Sci. Technol. Adv. Mater*. **10** 014604
[9] Fukushima T, Horii S, Uchikoshi T, Ogino H, Ishihara A, Suzuki T S, Sakka Y, Shimoyama J and Kishio K 2009 *IEEE Trans. Appl. Supercond.* **19** 2961
[10] Hiroi Z, Takano M, Takeda Y, Kanno R and Bando Y 1988 *Jpn. J. Appl. Phys.* **27** L580

[1] Wu M K, Ashburn J R, Torng C J, Hor P H, Meng R L, Gao L, Huang Z J, Wang Y Q, and Chu C W 1987 *Phys. Rev. Lett.* **58** 908.
[2] Kishio K, Shimoyama J, Kimura T, Kotaka Y, Kitazawa K, Yamafuji K, Li Q, and Suenaga M 1994 *Physica C* **235–240** 2775.
[3] Cardwell D A 1998 *Mater. Sci. Eng. B* **53** 1.
[4] Foltyn S R, Civale L, MacManus-Driscoll J L, Jia Q X, Maiorov B, Wang H, and Maley M 2007 *Nat. Mater.* **6** 631.
[5] Karpinski J, Kaldis E, Jilek E, Rusiecki S, and Bucher B 1988 *Nature* **336** 660.
[6] Marshall A F, Barton R W, Char K, Kapitulnik A, Oh B, Hammond R H, and Laderman S S 1989 *Phys. Rev. B* **37** 7347.
[7] Iye Y, Tamegai T, Takeya H, and Takei H 1987 *Jpn. J. Appl. Phys.* **26** L1057.
[8] Kishio K, Shimoyama J, Hasegawa T, Kitazawa K and Fueki K 1987 *Jpn. J. Appl. Phys.* **26** L1228
[9] Nakazawa Y, Ishikawa M, Takabatake T, Koga K, and Terakura K 1987 *Jpn. J. Appl. Phys.* **26** L796.
[10] Jorgensen J D, Veal B W, Paulikas A P, Nowicki L J, Crabtree G W, Claus H, and Kwok W K 1990 *Phys. Rev. B* **41** 1863.
[11] Welp U, Kwok W K, Crabtree G W, Vandervoort K G, and Liu J Z 1990 *Appl. Phys. Lett.* **57** 84.
[12] Hirschfeld P J, Wölfle P, Sauls J A, Einzel D, and Putikka W O 1989 *Phys. Rev. B* **40** 6695.
[13] Dimos D, Chaudhari P, and Manhart J 1990 *Phys. Rev. B* **41** 4038.
[14] Dimos D, Chaudhari P, Mannhart J and LeGoues F K 1988 *Phys. Rev. Lett.* **61** 219
[15] Laibowitz R B, Koch R H, Chaudhari P and Gambino R J 1987 *Phys. Rev. B* **35** 8821
[16] Sawano K, Morita M, Tanaka M, Sasaki T, Kimura K, Takebayashi S, Kimura M, and Miyamoto K 1991 *Jpn. J. Appl. Phys.* **30** 1153.
[17] Watanabe K, Awaji S, Fukase T, Yamada Y, Sakuraba J, Hata F, Chong C K, Hasebe T, and Ishihara M 1994 *Cryogenics* **34** 639.
[18] Watanabe K and Awaji S 2003 *J. Low Temp. Phys.* **133** 17.
[19] Ikezoe Y, Hirota N, Nakagawa J, and Kitazawa K 1998 *Nature* **393** 749.
[20] Stains M, Genoud J, Mawdsley A, and Manojlovic V 1999 *IEEE Trans. Appl. Supercond.* **9** 2284.
[21] Kimura T, Kimura F and Yoshino M 2006 *Langmuir* **22** 3464
[22] Fukushima T, Horii S, Ogino H, Uchikoshi T, Suzuki T S, Sakka Y, Shimoyama J and

Kishio K 2008 *Appl. Phys. Express* **1** 111701
[23] Horii S, Ishihara A, Fukushima T, Uchikoshi T, Ogino H, Suzuki T S, Sakka Y, Shimoyama J and Kishio K 2009 *Sci. Technol. Adv. Mater*. **10** 014604
[24] Yamaki M, Horii S, Haruta M, and Shimoyama J 2012 *Jpn. J. Appl. Phys.* **51** 010107.
[25] Song Y T, Peng J B, Wang X, Sun G L, and Lin C T 2007 *J. Cryst. Growth* **300** 263.
[26] Sun G L, Song Y T, and Lin C T 2008 *Supercond. Sci. Technol.* **21** 125001.
[27] Yamada Y, Jorgensen J D, Pei S, Lightfoot P, Kodama Y, Matsumoto T, and Izumi F 1991 *Physica C* **173** 185.
[28] Horii S, Yamada Y, Ikuta H, Yamada N, Kodama Y, Katano S, Funahashi Y, Morii S, Matsushita A, Matsumoto T, Hirabayashi I, and Mizutani U 1998 *Physica C* **302** 10.
[29] Miyatake T, Gotoh S, Koshizuka N, and Tanaka S 1989 *Nature* **341** 41.
[30] Funaki S, Yamada Y, and Nakayama F 2014 *J. Phys. Conf. Ser.* **507** 012016.
[31] Zheng X G, Suzuki M, Xu C, Kuriyaki H, and Hirakawa K 1996 *Physica C* **271** 272.
[32] Horii S, Yamaki M, Ogino H, Maeda T, and Shimoyama J 2010 *Physica C* **470** 1056.
[33] Horii S, Okuhira S, Yamaki M, Kishio K, Shimoyama J and Doi T 2014 *J. Appl. Phys.* **115** 113908.
[34] Ishihara A, Horii S, Uchikoshi T, Suzuki T S, Sakka Y, Ogino H, Shimoyama J, and Kishio K 2008 *Appl. Phys. Express* **1** 031701.
[35] Kupfer H, Wolf T, Zhukov A A, and Meier-Hirmer R 1999 *Phys. Rev. B* **60** 7631.
[36] Masui T, Takano Y, Yoshida K, Kajita K, and Tajima S 2004 *Physica C* **412–414** 515.

Figure Captions

Figure 1
Crystal structures of (a) Y123 and (b) Y124

Figure 2
(a) A secondary electron image of pulverised $(Y_{1-x}Ca_x)124$ (x = 0.1) powder; (b) schematic of the relationship among H_a, measured surfaces of XRD (α, β, γ), and rotation of a sample

Figure 3
Powder XRD patterns for $(Y_{1-x}Ca_x)124$ (T_k = 750°C)

Figure 4
Relationship between growth temperature and the grown phase for a nominal Ca-doping level of $(Y_{1-x}Ca_x)124$

Figure 5
(a) The χ-T curves for powders of $(Y_{1-x}Ca_x)124$ (T_k = 750°C); (b) the change in the T_c as a function of x for $(Y_{1-x}Ca_x)124$. The T_c values reported by Miyatake *et al*. [29] and Zheng *et al*. [31] are also shown for reference.

Figure 6
XRD patterns at the α, β, and γ planes for $(Y_{1-x}Ca_x)124$ powder samples oriented in the MRF of 10 T with (a) x = 0, (b) x = 0.05, and (c) x = 0.1

Figure 7
X-ray rocking curves at the (a) (00$\underline{12}$) and (b) (200) peaks for $(Y_{1-x}Ca_x)124$ (x = 0.1) powder samples oriented in the MRFs of 1, 5, and 10 T

Figure 8
Relationship between the degree of orientation and x for $(Y_{1-x}Ca_x)124$ powder samples oriented in the MRFs of 1, 5, and 10 T; (a) and (b) are results for the degrees of the c-axis and in-plane orientations.

Figure 9
Irreversibility lines (H//c) for $(Y_{1-x}Ca_x)124$ (x = 0, 0.05, and 0.1); ILs reported by Funaki *et al*. [30] and Kupfer *et al*. [35] are also shown for reference.

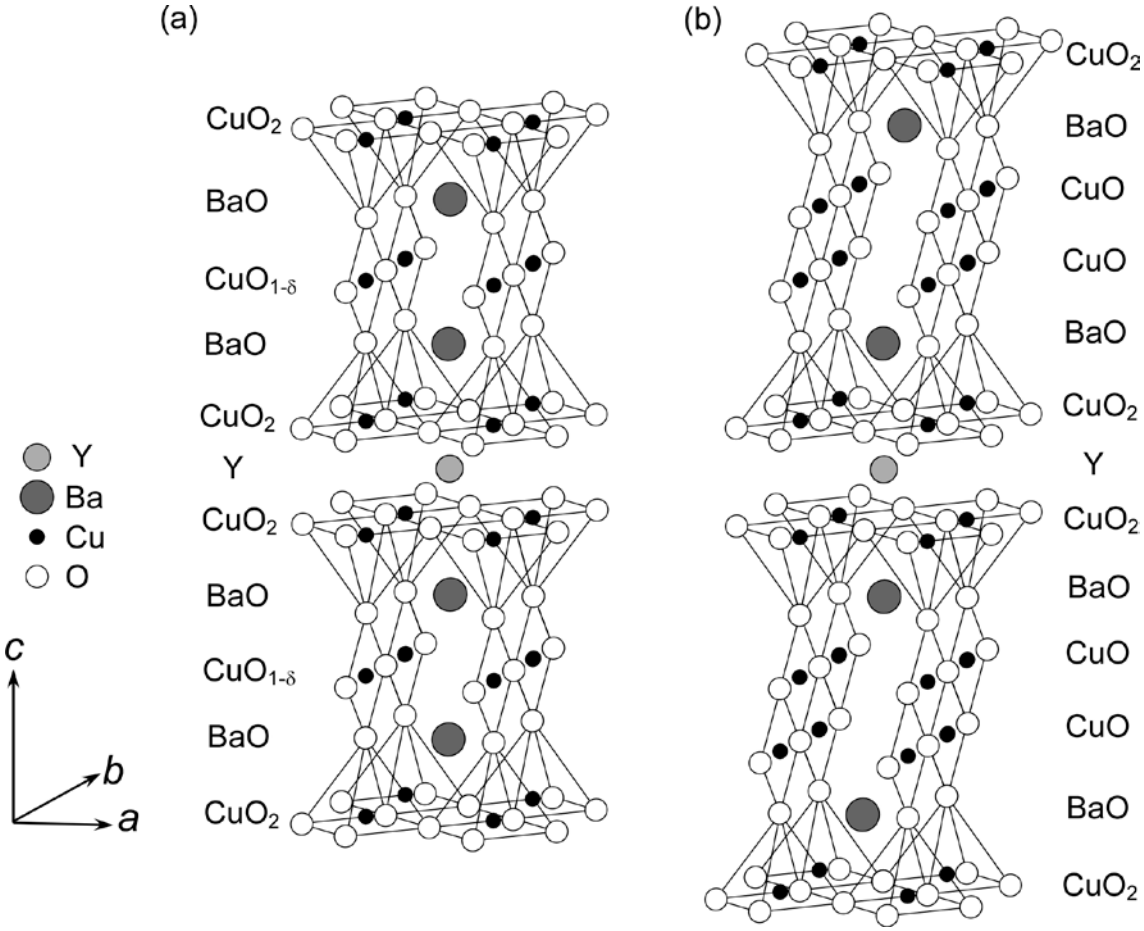

Figure 1 Horii *et al.*

(a)

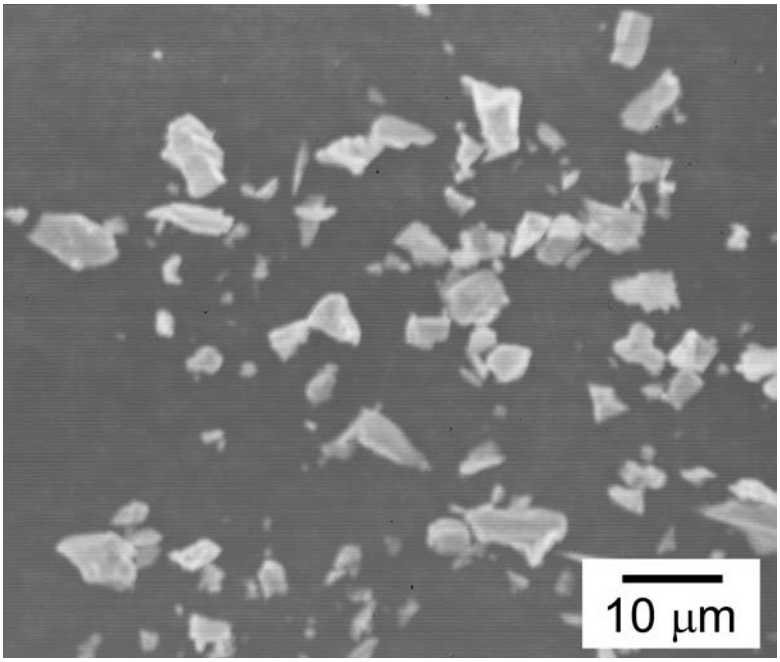

(b)

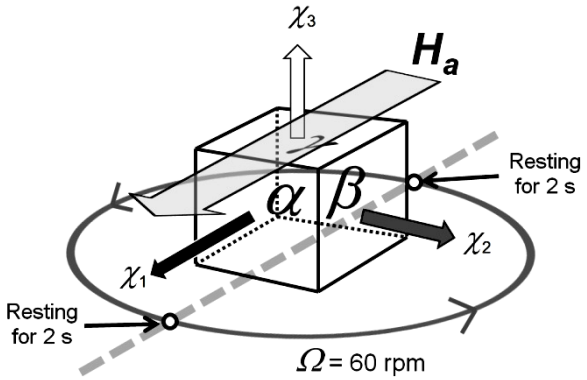

Figure 2 Horii *et al.*

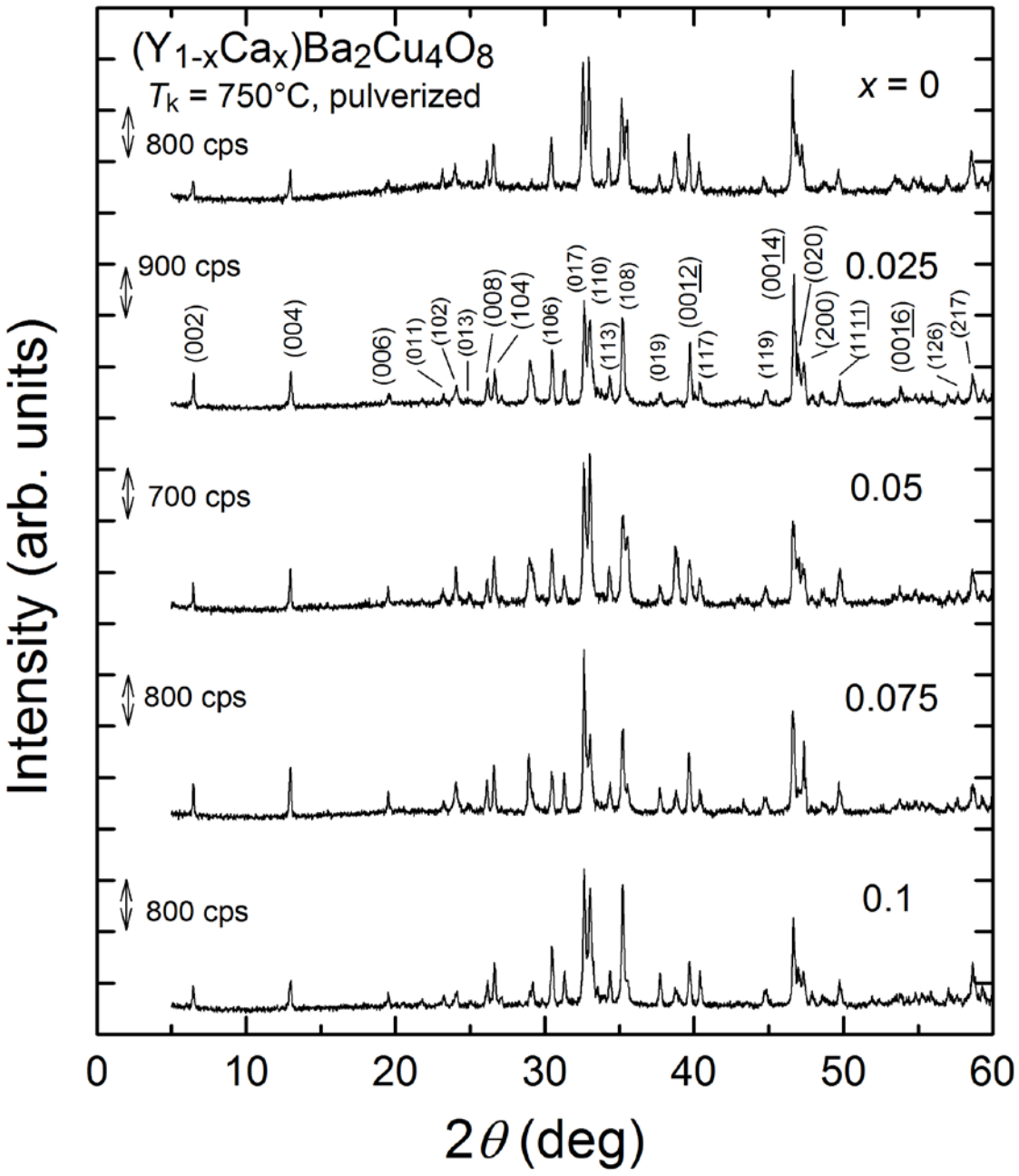

Figure 3 Horii et al.

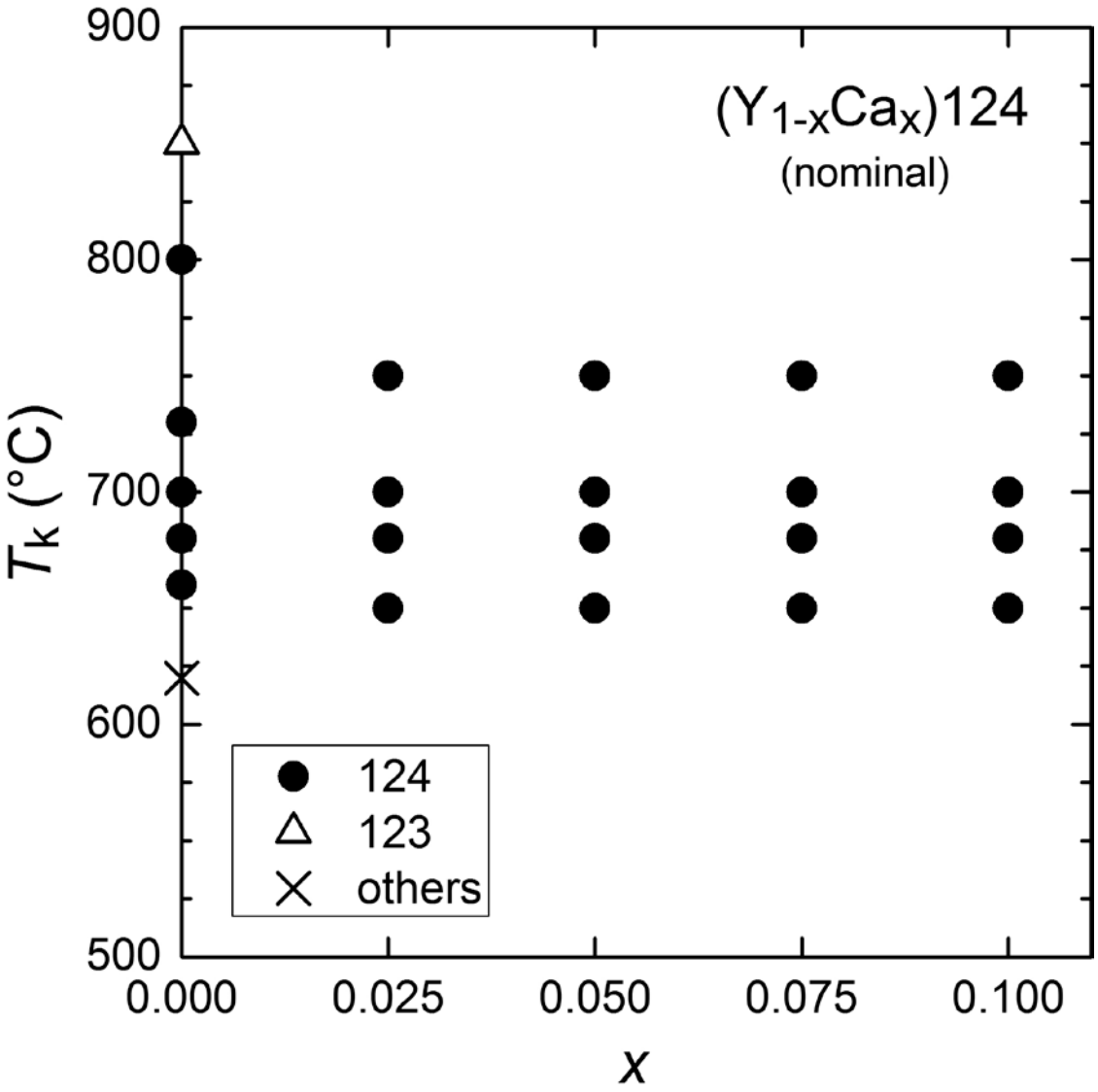

Figure 4 Horii *et al.*

(a)

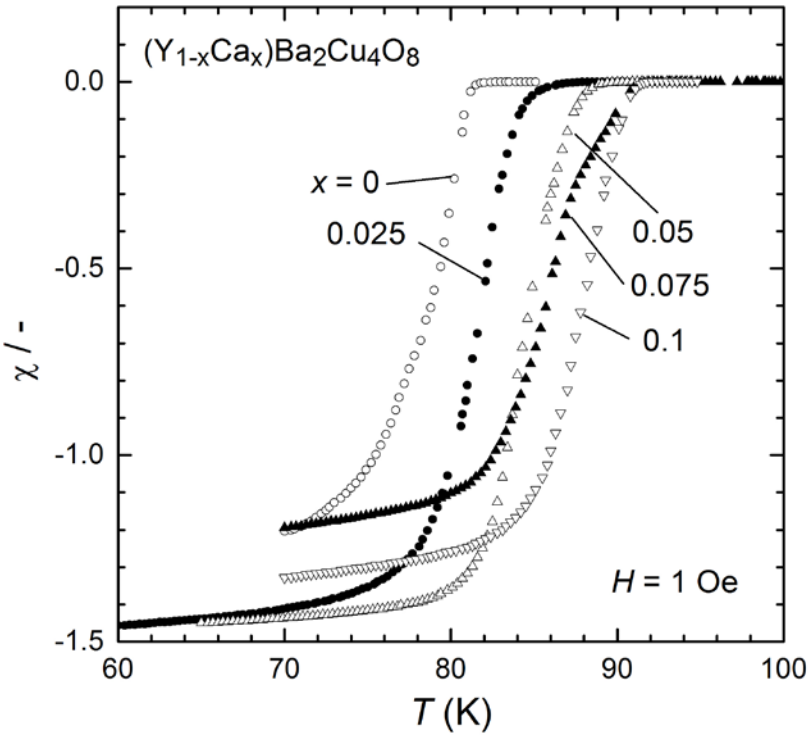

(b)

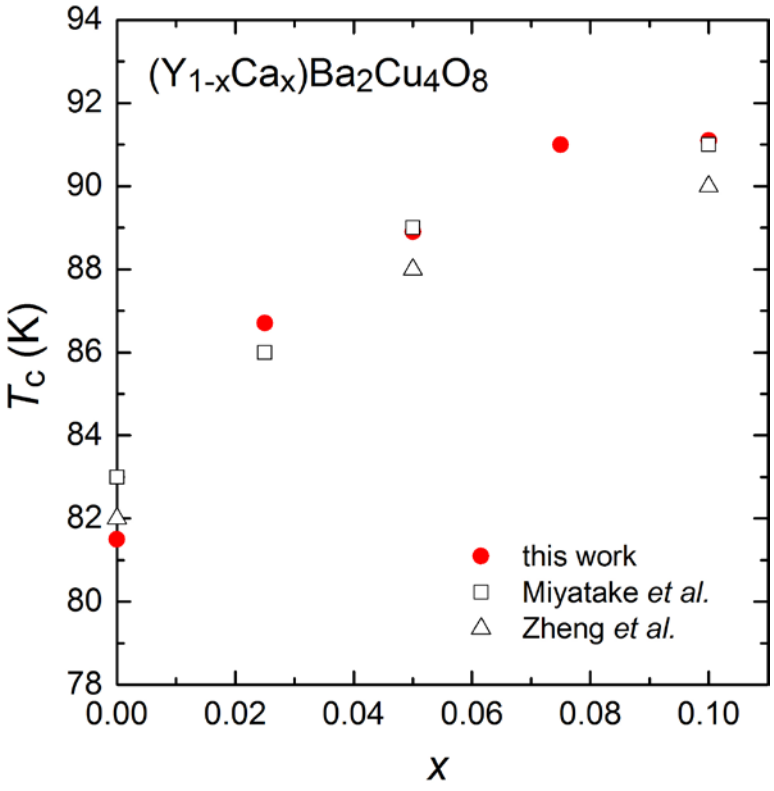

Figure 5 Horii *et al.*

(a)

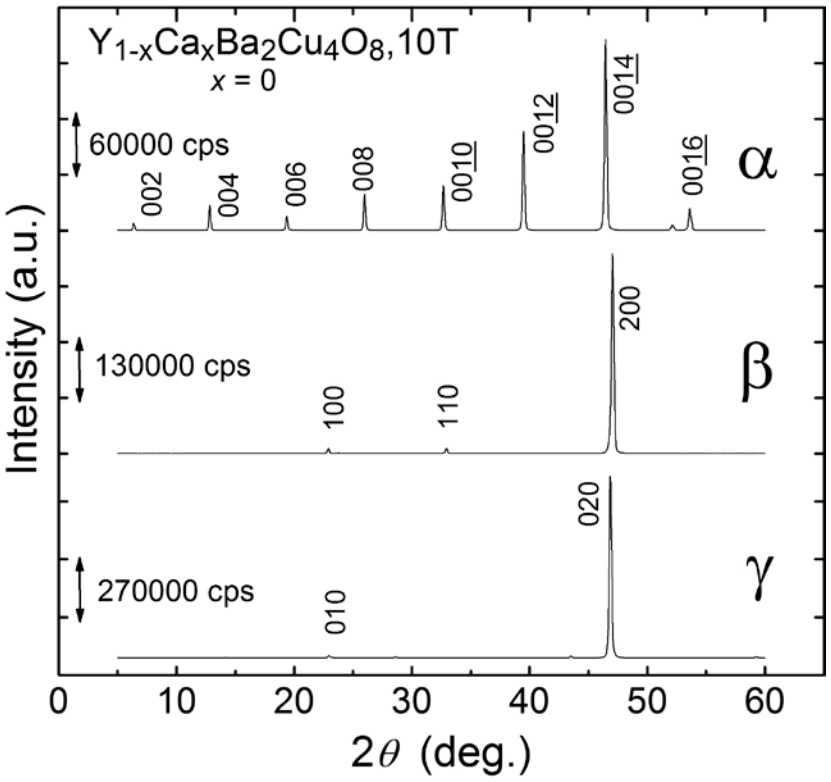

(b)

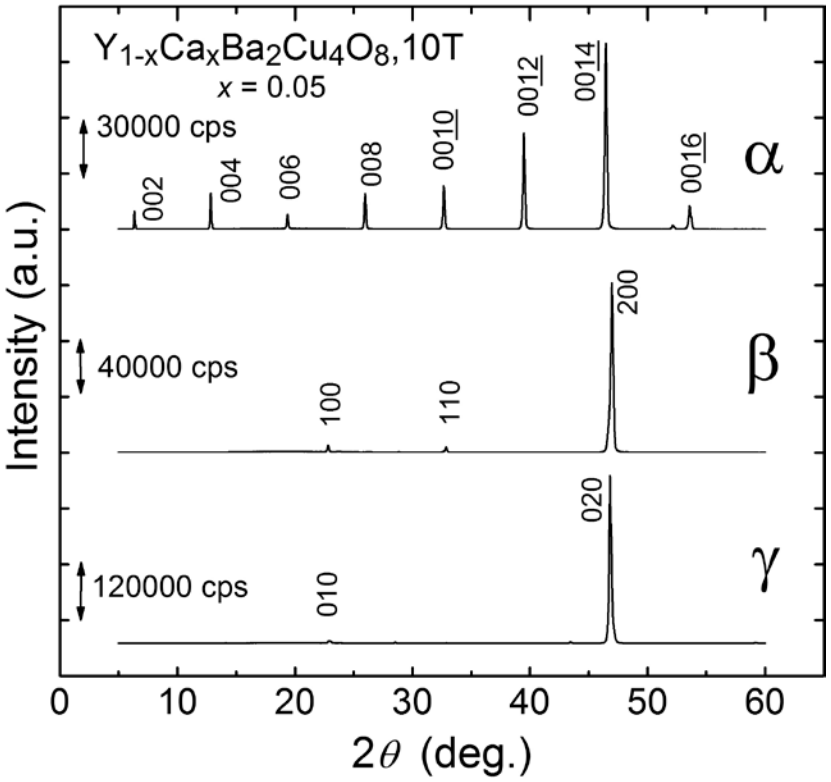

(c)

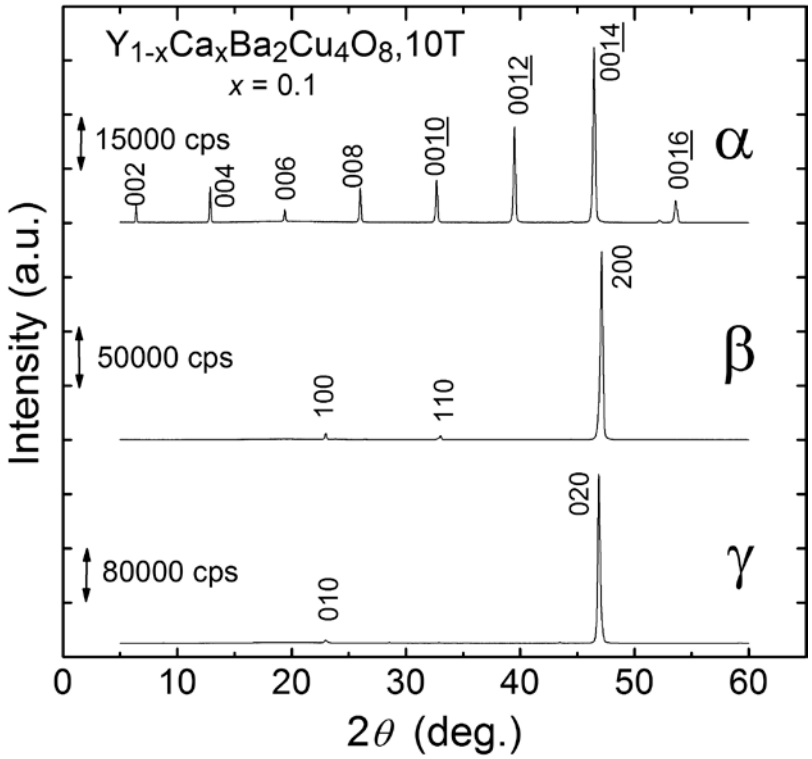

Figure 6 Horii *et al.*

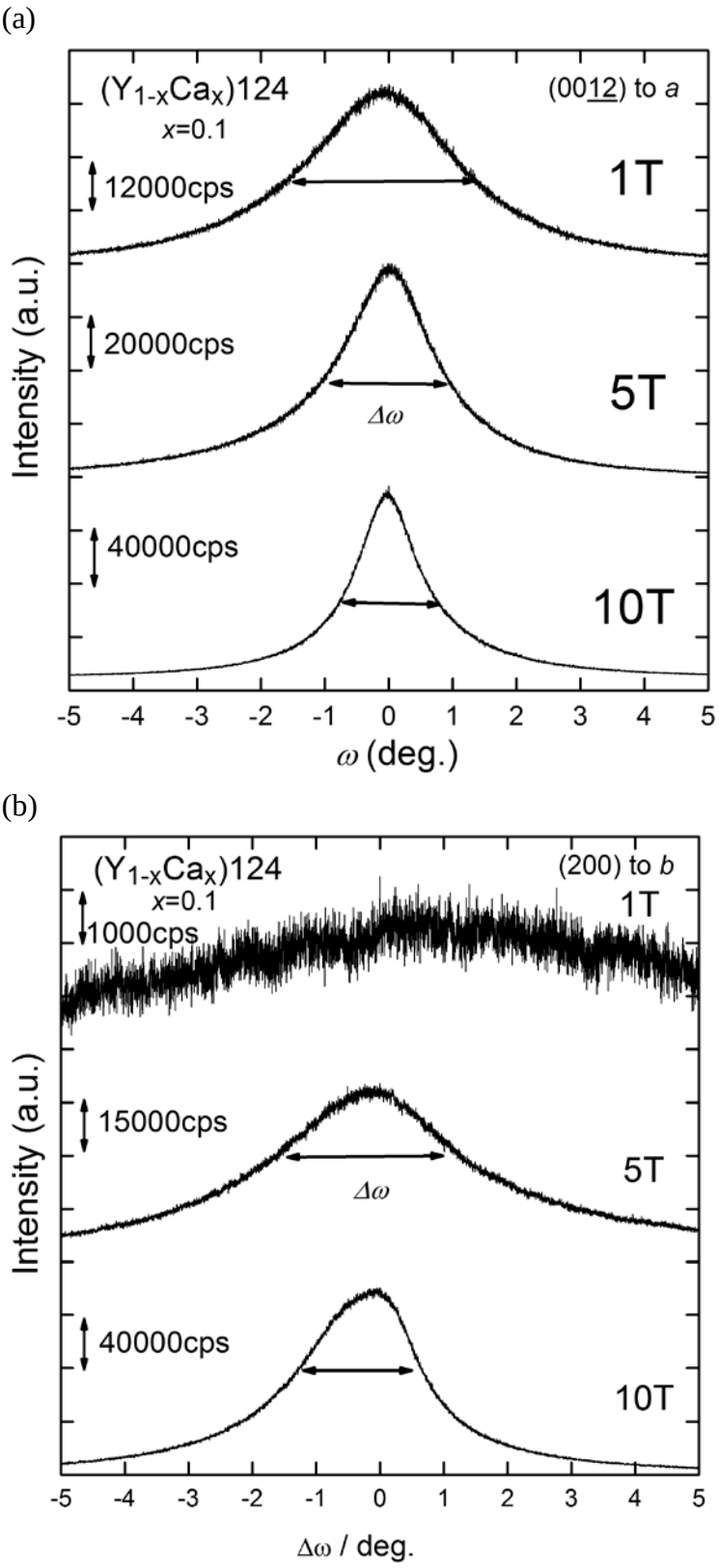

Figure 7 Horii *et al.*

(a)

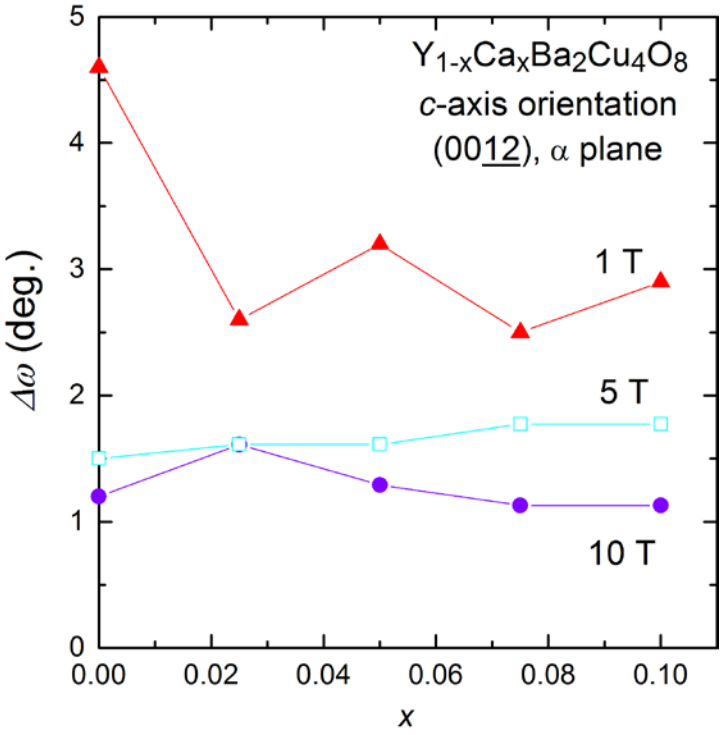

(b)

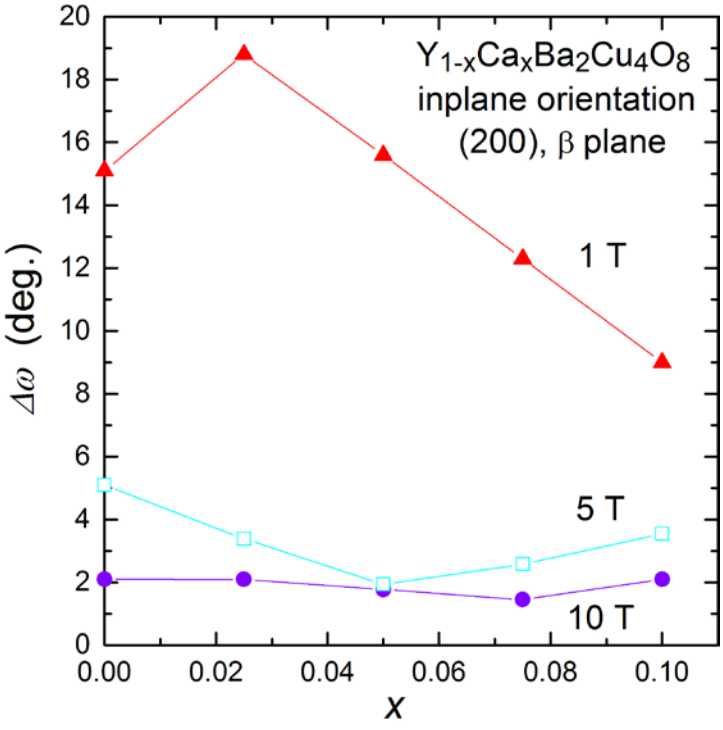

Figure 8 Horii *et al.*

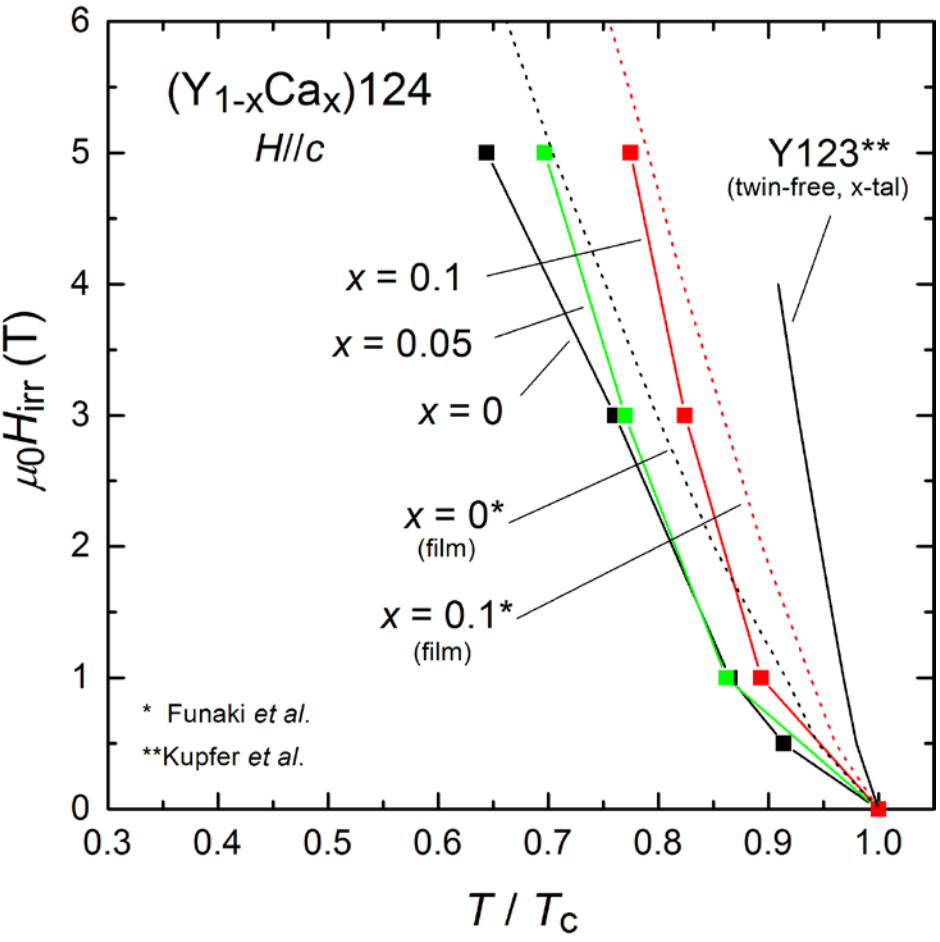

Figure 9 Horii *et al.*